

DOI: 10.1070/QEL16050

Ellipticity dependence of high harmonic yield in intense laser field: case of s-valence electron

T.S. Sarantseva, A.A. Silaev, N.V. Vvedenskii, M.V. Frolov, N.L. Manakov

Abstract. **Having solved numerically the time-dependent Schrödinger equation, we have analysed the dependence of the high harmonic generation yield on the ellipticity of an intense laser field. For the case of a zero angular momentum of an initial state, it has been shown that the ellipticity dependence of the HHG yield is affected by the harmonic number. The numerical results are interpreted in the framework of our recently developed quasi-classical analytical model for HHG. In the quasi-classical approximation, the difference in the ellipticity dependence of the HHG yield for different harmonics is shown to be caused by the interference effects of quantum orbits.**

Keywords: *femtosecond pulses, atoms, ionisation, high harmonic generation, attosecond pulses, numerical simulation.*

1. Introduction

High harmonic generation (HHG) occupies one of the central places in the physics of interaction of ultraintense laser fields with atomic and molecular systems. The presence of a characteristic plateau-like structure in the spectrum of high harmonics allows the use of HHG for producing attosecond laser pulses [1, 2]. Of special relevance is the task of obtaining an isolated attosecond pulse. One of the commonly used methods for the generation of such pulses is a polarisation gating technique [3–5], the essence of which consists in the fact that the polarisation parameters of the pump pulse are selected in such a way that the main contribution to the HHG amplitude is made by only one optical cycle of the pump field. As this takes place, the contributions from other cycles of the field are suppressed by increasing the ellipticity of the pump field. Using this technique of generation of isolated attosecond pulses requires a detailed analysis of the dependence of the HHG yield on the pump field ellipticity. This dependence has been investigated in several studies [6–8], the latter of which has shown that the dependence of the high harmonic yield on the laser pulse ellipticity is sufficiently universal and corresponds to a Gaussian distribution.

Qualitatively, the spectral features of high harmonics are described within the framework of a three-step rescattering model [9], in accordance with which the HHG process can be divided into three steps. In the first step, the valence electron of the atom tunnels through the barrier produced by an atomic potential and laser field. In the second step, the electron moves in a field-modified continuum and after some time returns to the parent ion, gaining additional energy from the laser field. Finally, in the third step, the electron recombines to the initial bound state, accompanied by the emission of fundamental radiation harmonics. As shown in [8, 10], a Gaussian dependence of the harmonic yield on the ellipticity is caused by the first step, i.e. tunnelling of the valence electron in an elliptically polarised laser field. At the same time, the effect of the second (propagation) and third (recombination) HHG steps on the law of a decrease in the harmonic yield with increasing ellipticity has not been studied. The aim of this work is to investigate the deviations of the dependence of the HHG yield with increasing laser field ellipticity on the Gaussian law, due to the peculiarities of the electron propagation in a laser-dressed continuum.

2. Numerical results for the HHG spectrum

Interaction of a laser field with an atom induces a dipole moment $[\boldsymbol{D}(t)]$, whose spectrum defines the probability of the harmonic generation [11]*:

$$\rho(\Omega) = \frac{\Omega^4}{4c^3}|\boldsymbol{D}(\Omega)|^2,\ \ \boldsymbol{D}(\Omega) = \frac{1}{\pi}\int_{-\infty}^{\infty}\boldsymbol{D}(t)\mathrm{e}^{\mathrm{i}\Omega t}\mathrm{d}t, \qquad (1)$$

where $\rho(\Omega)$ is the spectral density at frequency Ω; $\boldsymbol{D}(\Omega)$ is the Fourier transform of the dipole moment at frequency Ω; and c is the speed of light. In numerical calculations of the HHG spectra, instead of the dipole moment $\boldsymbol{D}(t)$ it is convenient to use the dipole acceleration $\boldsymbol{a}(t) = \ddot{\boldsymbol{D}}(t)$, the Fourier transform of which is related to $\boldsymbol{D}(\Omega)$ by the obvious expression:

$$\boldsymbol{a}(\Omega) = -\Omega^2\boldsymbol{D}(\Omega). \qquad (2)$$

Quantum mechanically (in the single-active-electron approximation) the dipole acceleration is calculated as an average value of the total force acting on the atomic electron in an intense laser field:

*In this paper we use atomic units.

T.S. Sarantseva, A.A. Silaev, N.V. Vvedenskii Institute of Applied Physics, Russian Academy of Sciences, ul. Ul'yanova 46, 603950 Nizhnii Novgorod, Russia; e-mail: vved@appl.sci-nnov.ru;
M.V. Frolov Institute of Applied Physics, Russian Academy of Sciences, ul. Ul'yanova 46, 603950 Nizhnii Novgorod, Russia; Voronezh State University, Universitetskaya pl. 1, 394006 Voronezh, Russia;
N.L. Manakov Voronezh State University, Universitetskaya pl. 1, 394006 Voronezh, Russia

Received 8 February 2016
Kvantovaya Elektronika **46** (4) 366–370 (2016)
Translated by I.A. Ulitkin

$$\boldsymbol{a}(t) = \int \psi^*(\boldsymbol{r},t)[-\boldsymbol{F}(t) - \nabla U(r)]\psi(\boldsymbol{r},t)\mathrm{d}r, \quad (3)$$

where $\psi(\boldsymbol{r},t)$ is the wave function of an electron in an atomic potential $U(r)$ and in the laser field with the electric vector $\boldsymbol{F}(t)$. The vector $\boldsymbol{F}(t)$ can be represented as

$$\boldsymbol{F}(t) = \frac{F_0}{\sqrt{1+\eta^2}} f(t)[\boldsymbol{e}_X\cos(\omega t) + \eta\boldsymbol{e}_Y\sin(\omega t)], \quad (4)$$

where F_0 is the peak electric vector; ω is the carrier frequency; η is the ellipticity; and the function $f(t)$ specifies the pulse envelope. To simplify the interpretation of the numerical results, in this paper we use a trapezoidal pulse with two full cycles in the regions of switching on/off the field and four full cycles in the region of a constant field amplitude:

$$f(t) = \begin{cases} t/(2T), & 0 < t \leqslant 2T, \\ 1, & 2T < t \leqslant 6T, \\ 1-(t-6T)/(2T), & 6T < t \leqslant 8T, \\ 0, & t \leqslant 0,\ t > 8T, \end{cases}$$

where $T = 2\pi/\omega$.

The exact wave function $\psi(\boldsymbol{r},t)$ satisfies the time-dependent Schrödinger equation (TDSE):

$$\mathrm{i}\frac{\partial\psi(\boldsymbol{r},t)}{\partial t} = \left[-\frac{\nabla^2}{2} + U(r) + \boldsymbol{r}\boldsymbol{F}(t)\right]\psi(\boldsymbol{r},t) \quad (5)$$

with the initial condition $\psi(\boldsymbol{r}, t=0) = \psi_0(\boldsymbol{r})$, where $\psi_0(\boldsymbol{r})$ is the ground state in the potential $U(r)$ with the angular momentum $l = 0$. The atomic potential is chosen in the form

$$U(r) = -b\,\mathrm{sech}^2(r/a) - \tanh(r/a)/r \quad (6)$$

with the parameters $a = 0.3$ and $b = 2.17$, providing the coincidence of energy of the ground s-states in the given potential with energy of the ground state of the hydrogen atom. Note that for large distances ($r \gg a$) the behaviour of potential (6) is determined a purely Coulomb dependence: $U(r) \approx -r^{-1}$.

For the numerical integration of TDSE (5) we employ a pseudospectral method using a fast Fourier transform algorithm in the directions x, y, z [12, 13]. The convergence of the numerical results is ensured by the selection of the integration grid size and the values of spatiotemporal steps: the number of nodes $N_x = 512$, $N_y = N_z = 256$ along each of the coordinate x, y and z, respectively; and the steps in time and coordinates $\Delta t = 0.025$, $\Delta x = \Delta y = \Delta z = 0.3$. To suppress spurious reflection waves, we use absorption layers of width 20 near the grid boundary along the coordinate x, and 15 – along the coordinates y and z.

To reduce pulse shape effects, we perform an averaging of the numerical results by calculating the integral yield of harmonics (R_N) in the vicinity of frequency $\Omega = N\omega$:

$$R_N = \int_{(N-1)\omega}^{(N+1)\omega} \rho(\Omega)\mathrm{d}\Omega, \quad \rho(\Omega) = |\boldsymbol{a}(\Omega)|^2/(4c^3), \quad (7)$$

To study the dependence of the HHG yield on the ellipticity η, we introduce the reduced HHG yield:

$$\hat{R}_N(\eta) = R_N(\eta)/R_N(\eta = 0). \quad (8)$$

Figure 1 shows the dependence of the reduced yield $\hat{R}_N$ on the harmonic number and ellipticity η for $\omega = 0.057$ (800 nm wavelength) and peak field strength $F_0 = 0.107$, corresponding to the peak intensity $I_0 = cF_0^2/(8\pi) = 4\times10^{14}$ W cm^{-2}. The numerical results show that at a fixed harmonic number, the reduced harmonic yield as a function of ellipticity η can be approximated by the expression:

$$\hat{R}_N(\eta) \approx (1 + f_N\eta^2)^2\mathrm{e}^{-\alpha\eta^2}, \quad (9)$$

where the superscript α is universal for all harmonics and the coefficient f_N, determining pre-exponential factor, essentially depends on the harmonic number, for example, for $N = 45$ (see Fig. 1) the distribution in η is determined with good accuracy by a purely Gaussian distribution; however, for $N = 47$ the reduced yield $\hat{R}_N(\eta)$ as a function of η decreases much faster. (Note that the violation of the Gaussian dependence $\hat{R}_N(\eta) \propto \exp(-\alpha\eta^2)$ for the harmonics in the region of a high-energy plateau is in contradiction with the quasi-classical result from paper [8].)

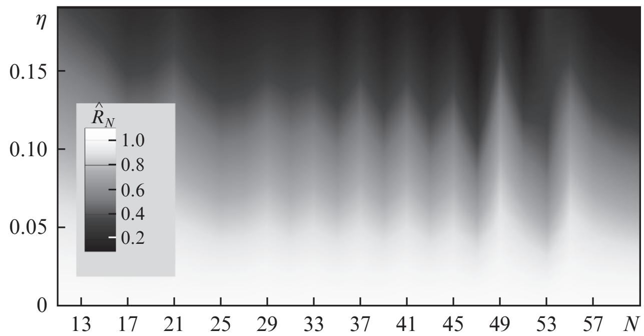

Figure 1. Dependence of the reduced harmonic yield in the region of the high-energy plateau on the ellipticity of a laser pulse with a carrier frequency $\omega = 0.057$ at a peak vector $F_0 = 0.107$.

3. Interpretation of the numerical results

To analyse qualitatively the high harmonic yield in the region of a high-energy plateau we will use the analytical approach proposed in [10] for an initial state having a zero angular momentum. According to this approach, the HHG yield near the high-energy plateau cutoff can be presented as the product of three factors, each of which has a clear physical meaning in terms of the three-step scenario [10]:

$$R_N(\eta) = I(\eta)\,W(E,\eta)\sigma(E,\theta = 0), \quad E = \Omega - I_\mathrm{p}, \quad (10)$$

where I_p is the ionisation potential of the ground state. The factor $I(\eta)$ describes the tunnelling of the bound electron in the elliptically polarised field, the factor $W(E)$ describes the propagation of the electron in the laser-dressed continuum, and the factor $\sigma(E,\theta)$ is the exact photorecombination cross section to the ground state $\psi_0(\boldsymbol{r})$ for the electron with energy E, which emits a photon with frequency $\Omega = N\omega$, and the linearly polarised vector, whose geometry is determined by an angle θ between the momentum vector of the recombining electron and the polarisation vector. Expression (10) explicitly shows that for the case of the s-state the reduced harmonic yield does not depend on the photorecombination cross section:

$$\hat{R}_N(\eta) = \hat{I}(\eta)\,\hat{W}(E,\eta), \tag{11}$$

$$\hat{I}(\eta) = \frac{I(\eta)}{I(\eta=0)}, \quad \hat{W}(E,\eta) = \frac{W(E,\eta)}{W(E,\eta=0)}. \tag{12}$$

Let us consider each term in turn.

The ionisation factor $I(\eta)$ describes tunnelling of an optically active electron from a bound state $\psi_0(\boldsymbol{r})$ to the continuum state with a zero momentum projection along the major axis of the polarisation ellipse and a projection $p_y = \eta\sqrt{2\varepsilon_0}$ along the minor axis of the polarisation ellipse, where $\varepsilon_0 = 3.17U_\mathrm{p}$, $U_\mathrm{p} = F_0^2/(4\omega^2)$. As shown in [10], the factor $I(\eta)$ can be presented in the form

$$I(\eta) = \frac{4\Gamma_\mathrm{st}(\tilde{F})}{\pi\kappa}(\gamma^2 + \delta\eta^2), \tag{13}$$

where $\gamma = \omega\kappa/F_0$ is the Keldysh parameter; $\kappa = \sqrt{2I_\mathrm{p}}$;

$$\delta = 1.585; \quad \tilde{F} = 0.95F_0(1 + \delta\eta^2/\gamma^2)^{-3/2};$$

and $\Gamma_\mathrm{st}(\tilde{F}) \propto \exp(-2\kappa^3/3\tilde{F})$ is the probability of decay in a static electric field with an effective strength $\tilde{F}$ [14]. The analysis shows that the dependence on the parameter η^2 in the limit of small ellipticity η is significant only in the exponent, whereas the η-dependence in pre-exponential factors can be neglected. In this approximation, by expanding the exponent in a series,

$$\frac{1}{\tilde{F}} \approx \frac{1}{F_0}\left(1 + \frac{3}{2}\delta\eta^2/\gamma^2\right),$$

we obtain the expression for the ionisation factor $I(\eta)$:

$$I(\eta) \approx I(\eta=0)\,\mathrm{e}^{-\alpha\eta^2}, \quad \alpha = \delta\kappa^3/(F_0\gamma^2). \tag{14}$$

Thus, the dependence of the reduced ionisation factor $\hat{I}(\eta) = I(\eta)/I(\eta=0)$ on ellipticity is determined by the Gaussian dependence [8, 10] and does not depend on the energy (or number) of the harmonic:

$$\hat{I}(\eta) \approx e^{-\alpha\eta^2}. \tag{15}$$

The propagation factor $W(E,\eta)$ in (10) describes the propagation of an electron in a laser-dressed continuum along closed classical trajectories and is expressed in terms of the Airy function $\mathrm{Ai}(x)$:

$$W(E,\eta) = \sqrt{2E}\,\rho^2\frac{\mathrm{Ai}^2(\zeta)}{(\Delta t)^3}, \tag{16}$$

where

$$\zeta = \zeta_0 + 0.83F_0^{-2/3}\varepsilon_0\eta^2, \tag{17a}$$

$$\zeta_0 = \rho(E - \varepsilon_0 - 0.324I_\mathrm{p}), \tag{17b}$$

$$\rho = (0.536F_0^2)^{-1/3}, \tag{17c}$$

$$\Delta t = 0.65T. \tag{17d}$$

It is known that in the region of photon energies close to the high-energy plateau cutoff, only two closed electron trajectories contribute to the amplitude of the HHG process [15]. Interference of these trajectories leads to an oscillation pattern in the HHG yield, which is described in (16) by the Airy function $\mathrm{Ai}(\zeta)$. Using (16), we obtain the expression for the reduced propagation factor:

$$\hat{W}(E,\eta) \approx \left(\frac{\mathrm{Ai}(\zeta_0 + \beta\eta^2)}{\mathrm{Ai}(\zeta_0)}\right)^2, \quad \beta = 0.83F_0^{-2/3}\varepsilon_0. \tag{18}$$

Let us analyse expression (18) in detail. In the case of small η, when expanding the Airy function in a series in η^2 up to terms of order η^2, it takes the form

$$\hat{W}(E,\eta) \approx \left[1 + \beta\eta^2\frac{\mathrm{Ai}'(\zeta_0)}{\mathrm{Ai}(\zeta_0)}\right]^2. \tag{19}$$

For further analysis of the ellipticity dependence of the HHG yield in the region of the high-energy plateau ($E < \varepsilon_0$) we use the asymptotics of the Airy function and its derivative and simplify expression (19) to the form:

$$\hat{W}(E,\eta) \approx (1 + f(E)\eta^2)^2, \tag{20}$$

where

$$f(E) = -\beta\sqrt{|\zeta_0|}\,\mathrm{ctg}\left(\frac{2}{3}|\zeta_0|^{3/2} + \frac{\pi}{4}\right). \tag{21}$$

For those arguments of ζ_0, which correspond to zeros of the Airy function, the value of $f(E)$ tends to infinity [see (18) and (19)]. The arguments ζ_0 can be found with high accuracy from Eqn (21) as roots, which leads to infinity of the cotangent in Eqn (21):

$$\zeta_n^{(\infty)} = -0.25[3\pi(4n+3)]^{2/3}, \quad n = 0,1,2,\ldots \tag{22}$$

This nonphysical behaviour for $\hat{W}$ at $\zeta_0 \to \zeta_n^{(\infty)}$ explicitly shows the limit of applicability of the analytical expression (10). The coefficient $f(E)$ becomes equal to zero at ζ_0 for which the cotangent in (21) vanishes:

$$\zeta_n^{(0)} = -0.25[3\pi(4n+1)]^{2/3}, \quad n = 0,1,2,\ldots \tag{23}$$

We note that conditions (22) and (23) correspond to those of destructive and constructive interference of short and long classical trajectories of an electron in a linearly polarised field [16].

Analytical results (15) and (20) for reduced ionisation and propagation factors allow us to study the ellipticity dependence of the reduced HHG yield for different N. As was already mentioned, the reduced ionisation factor (15) defines the universal (independent of N) Gaussian dependence of the reduced harmonic yield on η. Thus, the difference in the ellipticity dependence of the HHG yield for different N is caused by the dependence of the propagation factor on both the ellipticity η and harmonic energy. Obviously, for two harmonics with numbers N and N', for which the reduced propagation factors are related as $(\hat{W}(E_N,\eta) > \hat{W}(E_{N'},\eta))$ $(E_N = N\omega - I_p)$, the distribution of the reduced harmonic yield on η will be wider for the Nth harmonic than for the harmonic with the number N'.

Analytical results (20) allow one to establish a number of common features in the behaviour of $\hat{W}(E,\eta)$ and $\hat{R}_N(\eta)$. Consider a sequential set of harmonics, for which the ζ_0 values satisfy the inequality $\zeta_{n+1}^{(\infty)} < \zeta_0 < \zeta_n^{(\infty)}$. (Recall that with increasing energy of harmonics in the region of the high-energy plateau, the absolute value of ζ_0 decreases and remains negative [see the dependence of ζ_0 on the harmonic energy in (17b)].) In accordance with (20), for this group of harmonics the largest and smallest value of $f(E)$ will correspond to harmonics with the lowest and highest N, respectively. Thus, the yield of harmonics with the lowest energy will fall with increasing η slower than that for the harmonic with the highest energy. Indeed, in Fig. 1 the yield of the 45th harmonic with an increase in η decays much more slowly than the yield of the 47th harmonic. Let us now consider a group of harmonics for which ζ_0 values satisfy the inequality $\zeta_{n+1}^{(0)} < \zeta_0 < \zeta_n^{(0)}$. In this case, part of the harmonics have an energy that is smaller than the 'threshold' energy corresponding to $\zeta_n^{(\infty)}$, and the other – greater. In passing through threshold energy the sign of $f(E)$ is changed from negative to positive, leading to a change in the distribution of $\hat{R}_N$ with respect to η from narrow to a broader one; for example, in Fig. 1 the probability of the yield of the 51st harmonic decays much more rapidly with increasing η than that of the 55th harmonic. Thus, the transition from one harmonic to the other changes the dependence of the reduced harmonic yield on the field ellipticity, which leads to the emergence of an irregular behaviour of the numerically found dependence of $\hat{R}_N$ on η and N in Fig. 1.

Figure 2 shows the reduced HHG yield near the high-energy plateau cutoff for the same parameters of the laser field, as those in Fig. 1. The colour scale (from light to dark) shows the results of the numerical solution of the TDSE, and the level lines correspond to the analytical results (11). As can be seen from Fig. 2, the analytical results are in good agreement with the results of the numerical solution of the TDSE with the exception of the harmonics near the region of destructive interference of short and long classical trajectories, for which, as noted above, the presented theory does not adequately describe the reduced yield $\hat{R}_N$. The energies of these harmonics are found from formula (22) with (17b) taken into account. The corresponding harmonic numbers are generally not integers and depend on the parameters of the laser field; therefore, Fig. 2 does not show the level lines in the vicinity of the harmonics with N = 43 and 53, for which the energies are close to the energies corresponding to the position of the dashed lines. However, in the vicinity of the harmonic with N = 47 the analytical results are in good agreement with the numerical ones, because the energy corresponding to the dashed line gives the value of N that is substantially different from the integer.

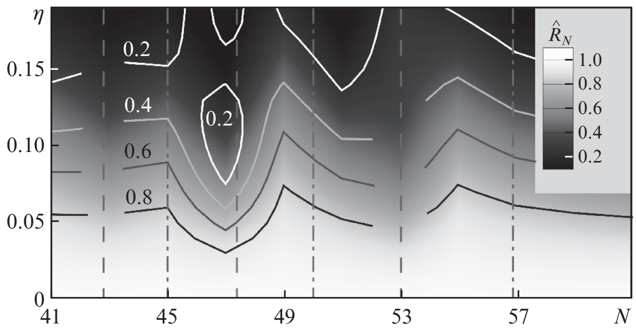

Figure 2. Dependence of the reduced HHG yield [see expression (8)] near the high-energy plateau cutoff on the ellipticity and harmonic number. Shown are the values of N (generally non-integer) satisfying the conditions of destructive (dashed lines) [see (22)] and constructive (dash-dotted lines) [see (23)] interference. The laser field parameters are the same as in Fig. 1.

4. Conclusions

We have studied the dependence of the HHG yield on the ellipticity of the external laser field for the case of HHG by an electron located initially in the s-state. It is shown that the law of a decrease in the yield of high harmonics with increasing ellipticity is not universal for the harmonics in the plateau region. Deviations of this law from the universal Gaussian distribution are associated with the interference of electron trajectories in the laser field, taking place in the second step of the quasi-classical HHG scenario, i.e. the step of the electron propagation in the continuum.

Thus, we have shown that the dependence of the HHG yield on the ellipticity of the pump field polarisation is not determined by the ionisation step only, as was assumed previously [8]. It should be noted that in the above-considered case of the s-valence electron the dependence of the reduced HHG yield on the atomic target parameters is absent. However, in the more general case of the nonzero angular momentum in an initial state, the effect of the atomic structure on the ellipticity dependence of the HHG yield can be more significant and requires a separate study.

Acknowledgements. This work was supported by the Russian Science Foundation (Grant No. 15-12-10033).

References

1. Corkum P.B., Krausz F. *Nature Phys.*, **3**, 381 (2007).
2. Krausz F., Ivanov M.Yu. *Rev. Mod. Phys.*, **81**, 163 (2009).
3. Corkum P.B., Burnett N.H., Ivanov M.Yu. *Opt. Lett.*, **19**, 1870 (1994).
4. Sansone G., Benedetti E., Calegari F., Vozzi C., Avaldi L., Flammini R., Poletto L., Villoresi P., Altucci C., Velotta R., et al. *Science*, **314**, 443 (2006).
5. Sansone G., Poletto L., Nisoli M. *Nature Photon.*, **5**, 655 (2011).
6. Kanai T., Minemoto S., Sakai H. *Phys. Rev. Lett.*, **98**, 053002 (2007).
7. He F., Ruiz C., Becker A. *Opt. Lett.*, **32**, 3224 (2007).
8. Möller M., Cheng Y., Khan S.D., Zhao B., Zhao K., Chini M., Paulus G.G., Chang Z. *Phys. Rev. A*, **86**, 011401R (2012).

9. Corkum P.B. *Phys. Rev. Lett.*, **71**, 1994 (1993).
10. Frolov M.V., Manakov N.L., Sarantseva T.S., Starace A.F. *Phys. Rev. A*, **86**, 063406 (2012).
11. Frolov M.V., Manakov N.L., Popov A.P., Tikhonova O.V., Volkova E.A., Silaev A.A., Vvedenskii N.V., Starace A.F. *Phys. Rev. A*, **85**, 033416 (2012).
12. Silaev A.A., Vvedenskii N.V. *Phys. Rev. Lett*., **102**, 115005 (2009).
13. Frolov M.V., Manakov N.L., Sarantseva T.S., Silaev A.A., Vvedenskii N.V., Starace A.F. *Phys. Rev. A*, **93**, 023430 (2016).
14. Smirnov B.M., Chibisov M.I. *Zh. Eksp. Teor. Fiz.*, **49**, 841 (1965).
15. Lewenstein M., Balcou P., Ivanov M.Yu., L'Huillier A., Corkum P.B. *Phys. Rev. A*, **49**, 2117 (1994).
16. Frolov M.V., Manakov N.L., Sarantseva T.S., Starace A.F. *J. Phys. B*, **42**, 035601 (2009).